PLC-based three-mode multi/demultiplexer for mode division multiplexing transmission

N. Hanzawa[1], K. Saitoh[2], T. Sakamoto[1], T. Matsui[1], K. Tsujikawa[1], T. Uematsu[2], M. Koshiba[2], and F. Yamamoto[1]

[1] NTT Access Network Service Systems Laboratories, Tsukuba, Ibaraki, Japan,
hanzawa.nobutomo@lab.ntt.co.jp
[2] Hokkaido University, Sapporo, Hokkaido, Japan,

Abstract: We realized a three-mode multi/demultiplexer (MUX/DEMUX) using parallel waveguides with a uniform height for mode division multiplexing transmission. We achieved the mode coupling of the LP_{01} mode to the LP_{21} mode by using the $LP_{11}b$ mode, which we generated by rotating the waveguide 90 degrees with the mode coupling of the LP_{01} mode to the $LP_{11}a$ mode. The mode conversion of the LP_{01} mode to the LP_{11} and LP_{21} modes in the C-band was achieved using our fabricated MUX/DEMUX.

Introduction: The transmission capacity in single-mode fiber (SMF) achieved by employing wavelength division multiplexing (WDM) and a multi-level modulation format is limited to around 100 Tbps owing to the input power and bandwidth limitations of an optical amplifier as shown in Fig. 1.[1] Recently, space division multiplexing (SDM) transmission with multi-core fiber and mode division multiplexing (MDM) transmission using few-mode fibers have been intensively studied and are attracting a lot of interest because of their potential for improving transmission capacity.[2-4] An optical fiber and a mode multi/demultiplexer (MUX/DEMUX) are the key components for realizing an MDM transmission. A mode MUX/DEMUX compatible with the LP_{21} mode has been realized using free space optics.[5]

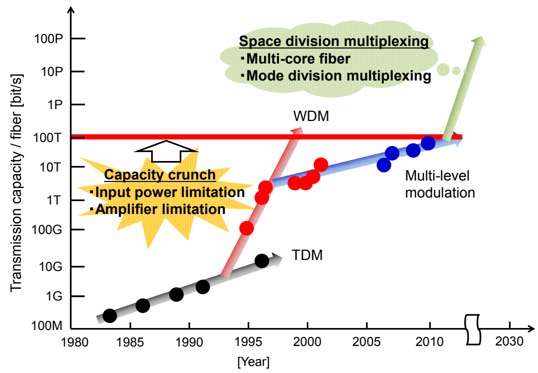

Fig. 1: Increase in single-mode fiber capacity.

We have already proposed a silica-based PLC-type two-mode MUX/DEMUX with a low insertion loss and a wide wavelength range.[6,7] The PLC-type device has distinctive advantages such as a small size, a high yield rate, and a low cost. Therefore, in terms of mass production, the use of a PLC with a uniform height as a mode MUX/DEMUX is a very promising approach, especially as the number of modes increases. In this paper, we report on a three-mode MUX/DEMUX for LP_{21} mode conversion. It was designed and fabricated using parallel waveguides with a uniform height.

Design of mode MUX/DEMUX for LP_{21} mode: Figure 2 shows the structure of our proposed three-mode MUX/DEMUX. The basic concept is the same as for LP_{21} mode coupling. Since the LP_{01} mode cannot be directly coupled to the $LP_{21}a$ mode by matching the effective index, it was realized by using the $LP_{11}b$ mode. The $LP_{11}b$ mode is generated by rotating the $LP_{11}a$ mode 90 degrees since it is also impossible to couple the LP_{01} mode to the $LP_{11}b$ mode. The LP_{01} mode from port 1 is converted to the $LP_{11}a$ mode, and the LP_{01} mode from port 2 is directly output at the output port. The LP_{01} mode from port 3 is converted to the $LP_{11}a$ mode, and the $LP_{11}b$ mode is generated from this $LP_{11}a$ mode by rotating the waveguide 90 degrees,

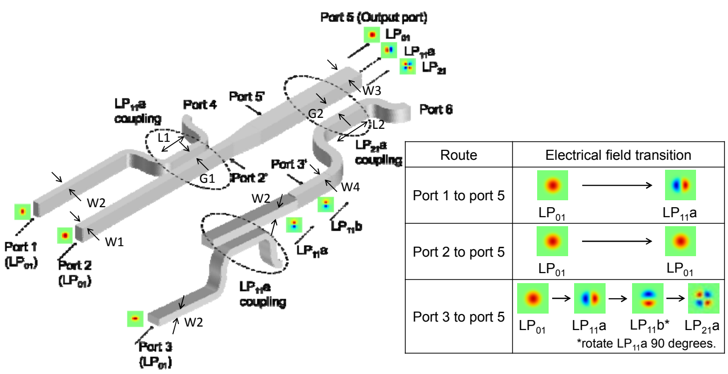

Fig. 2: Diagram of fabricated three-mode MUX/DEMUX.

which is converted to the LP_{21}a mode. Here, we assumed the relative index difference and the waveguide height to be 0.45% and 9.0 µm, respectively. We then calculated the mode coupling ratios of the LP_{01} mode to the LP_{11}a mode and the LP_{11}b mode to the LP_{21}a mode with three-mode multiplexing when we adopted w1, w2, w3, w4, G1, G2, L1, and L2 values of 12.9 µm, 4.5 µm, 19.1 µm, 7.0 µm, 4.0 µm, 9.0 µm, 0.65 mm, and 8.9 mm, respectively. Figure 3(a) and (b) show the wavelength dependence of the coupling ratios from port 1 or 2 to port 2' and from port 3' or 5' to port 5. The solid and dashed lines, respectively, show the coupling ratios of the LP_{01} and LP_{11}a modes in Fig. 3(a) and those of the LP_{11}a and LP_{21}a modes in Fig. 3(b). The coupling ratios of the LP_{11}a and LP_{21}a modes exceeded 98% and 92%, respectively, between 1530 and 1560 nm. We consider the mode crosstalk to be relatively small since the coupling ratios of the LP_{01} and LP_{11}a modes in a straight port exceeded 99%.

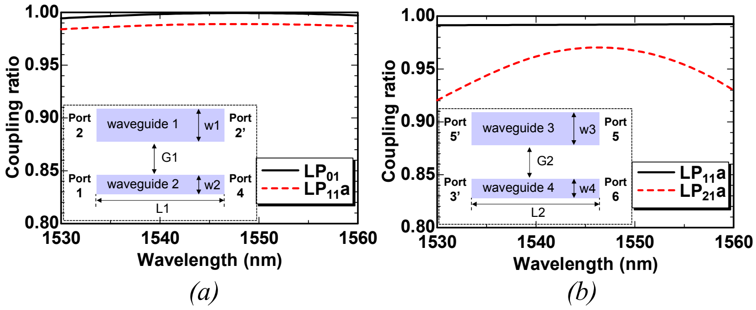

Fig. 3: (a) LP_{11}a mode coupling ratio dependence on wavelength. (b) LP_{21}a mode coupling ratio dependence on wavelength.

Experimental results: We fabricated three-mode MUX/DEMUXs using the above parameters. In the experiment, a four-mode fiber supporting the LP_{01}, LP_{11}, LP_{21}, and LP_{02} modes in the C-band was connected to the output port of the PLC, and a conventional SMF was connected to ports 1, 2, and 3. Figure 4 shows near field patterns (NFPs) measured at the output port when a CW light with a wavelength between 1530 and 1565 nm was input into ports 1, 2, and 3. The LP_{11} and LP_{21} mode patterns were clearly observed by converting the LP_{01} mode from ports 1 and 3 to the LP_{11} and LP_{21} modes in the waveguide. As a result, we confirmed that the three modes were multiplexed by the fabricated MUX/DEMUX in the C-band.

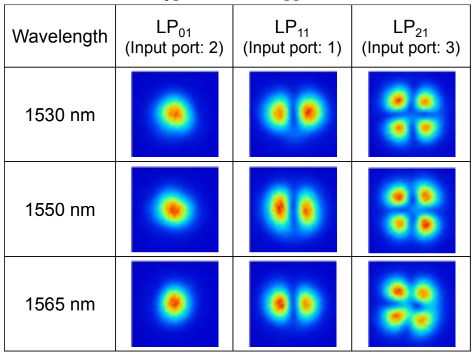

Fig. 4: NFP of output port from each input port.

We then observed the three-mode multi/demultiplexing. Figure 5 shows the eye patterns when the signals of an individual mode and three multiplexed modes were input into the three-mode DEMUX. Here, we used a 10 Gbps NRZ signal with a $2^{31}-1$ PRBS. The first, second, and third rows in Fig. 5 are the eye patterns of the LP_{01}, LP_{11}, and LP_{21} modes, respectively. Although the eye patterns of the third column were slightly degraded compared with those when the individual modes were input into the mode DEMUX, we confirmed that we could obtain relatively clear eye patterns with our fabricated three-mode DEMUX.

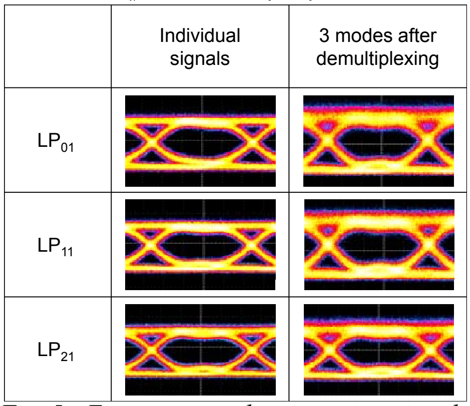

Fig. 5: Eye patterns when inputting signals of individual modes and three multiplexed modes.

Conclusions: We designed and fabricated a multi/demultiplexer for LP_{01}, LP_{11}, and LP_{21} mode conversion operating in the C-band using a silica-based PLC with a uniform height.

References

1. T. Morioka et al., IEEE Comm. Mag. **50**, p.s31-s42, (2012).
2. T. Mizuno et al., Proc. OFC2014, Th5B.2, (2014).
3. V.A.J.M. Sleiffer et al., Opt. Express, **20**, pp. B428-B438, (2012).
4. R. Ryf et al., Proc. OFC2013, PDP5A.1, (2013).
5. G. L. Cocq et al., Opt. Express **20**, pp. 27051-27061, (2012).
6. N. Hanzawa et al., Opt. Express **21**, pp. 25752-25760, (2013).
7. T. Uematsu et al., Proc. OFC2013, OTh1B.5, (2013).